Experimental Investigation of Laminar Burning Velocity of Methyl Acetate/Air Mixtures at Elevated Temperatures

Amardeep Fulzele, Vijay Shinde, Anshul & Sudarshan Kumar

View supplementary material

Published online: 30 Jul 2025.

Submit your article to this journal

View related articles

View Crossmark data

Check for updates

Experimental Investigation of Laminar Burning Velocity of Methyl Acetate/Air Mixtures at Elevated Temperatures

Amardeep Fulzele[a], Vijay Shinde[b], Anshul[c], and Sudarshan Kumar[a]

[a]Department of Aerospace Engineering, Indian Institute of Technology Bombay, Mumbai, India; [b]Department of Mechanical Engineering, K. J. Somaiya School of Engineering, Mumbai, India; [c]Department of Mechanical Engineering, National Institute of Technology, Hamirpur, India

ABSTRACT

The chemical kinetics of small alkyl esters provide a foundational basis for understanding the behavior of larger alkyl esters, which are key constituents of practical biodiesel fuels used in advanced internal combustion engines. This study presents experimental investigations on the laminar burning velocity (LBV) of methyl acetate/air mixtures over an elevated temperature range of 367 - 714 K and equivalence ratios (ϕ) from 0.7 to 1.4, using the externally heated diverging channel method under atmospheric pressure. The experimental results are evaluated against existing data and detailed chemical kinetic models developed by Ahmed (2019), Lubrano Lavadera (2022), and Diévart (2013). The present measurements show good agreement with previously reported values across a wide range of operating conditions. Kinetic models by Ahmed (2019) and Lubrano Lavadera (2022) accurately capture the LBV trends, particularly at elevated temperatures, while the Diévart (2013) model consistently overpredicts LBV under fuel-rich conditions. Across all temperatures, the LBV follows a parabolic trend with a maximum at a slightly rich equivalence ratio ($\phi = 1.1$), which is also predicted by the models. At $\phi = 1.0$, the LBV increases by approximately 97% as the temperature rises from 450 K to 650 K, while the peak LBV increases by about 86% from 500 K to 700 K, indicating a strong temperature dependence. Sensitivity analysis highlights the dominant role of reactions involving C_0 - C_4 species in governing the combustion behavior of methyl acetate/air mixtures.

Introduction

The increasing dependence on fossil fuel combustion has raised major concerns regarding climate change, energy security, and environmental pollution. Global energy demand is continuously rising, with fossil fuels remaining the dominant energy source worldwide (World Energy Outlook 2024). The ongoing reliance on fossil fuels has caused a consistent increase in carbon dioxide (CO_2) emissions in recent decades, playing a major role in the accumulation of greenhouse gases and resulting in global warming (Rial 2024). The depletion of oil reserves, growing energy consumption, and the environmental impact of conventional fuel emissions have driven a transition toward greener energy alternatives that are economical, low-emission, efficient, sustainable, and renewable (Sikiru et al. 2024).

Among such alternatives, biodiesel has emerged as a promising alternative to fossil fuels, particularly in the transportation sector (Oppong et al. 2022). Biofuels are widely regarded as practical and sustainable liquid fuel options, playing a significant role in promoting sustainable development by addressing both environmental and socioeconomic challenges (Coniglio et al. 2013). Their widespread availability enhances energy security in both developed and developing countries, while also providing rural communities with access to modern energy and generating employment opportunities (Coniglio et al. 2013). Compared to conventional fuels, biodiesel is a cleaner-burning alternative that emits lower levels of net CO_2, unburned hydrocarbons, carbon monoxide (CO), and particulate matter, while being free of sulfur oxides (Culaba et al. 2023). Biodiesel is primarily composed of methyl esters, which are alternative fuel components derived from renewable resources such as microalgae, vegetable oils, and animal fats through the transesterification process (Oppong et al. 2022).

Biofuels can be blended with conventional fuels with minimal or no modifications to existing engines. However, the combustion characteristics of biodiesels differ from those of conventional hydrocarbons. Therefore, comprehensive studies on their combustion mechanisms are essential prior to their use, either as pure fuels or in blends, in current engine systems. Biodiesels are typically composed of long-chain methyl esters, mainly in the C_{16} to C_{18} range (Lam, Davidson, and Hanson 2012). Due to their complex molecular structures, small methyl esters are commonly employed as surrogate fuels in both experimental and theoretical combustion studies (Lai, Lin, and Violi 2011). Investigating these smaller surrogates provides valuable insights into biodiesel oxidation processes and enhances our understanding of their combustion behavior in comparison to conventional fuels (Tan et al. 2015). Moreover, small esters often serve as intermediate species in the oxidation of larger esters and biodiesel. As such, a thorough understanding of their combustion characteristics is essential for accurately analyzing the combustion performance of biodiesel and its components.

The development of biodiesel and large ester combustion models depends heavily on the formulation of accurate kinetic models for small esters (Konnov, Chen, and Lubrano Lavadera 2023). To evaluate the impact of biofuels, whether used as pure components or blended with conventional fuels, on engine performance, their combustion behavior can be studied using computational fluid dynamics combined with detailed chemical kinetic models (Curran 2019). These models should be validated against key global combustion parameters such as major species time profiles, laminar burning velocity (LBV), and ignition delay times (IDTs) (Curran 2019).

Among the small alkyl esters, methyl acetate serves as a key surrogate component for biodiesel and also acts as a reaction intermediate during the pyrolysis of biodiesels (Osswald et al. 2007). Over the years, various researchers have conducted both modeling and experimental studies on methyl acetate due to its relevance in alternative fuels, emissions reduction, and chemical kinetics. These studies have focused on its combustion behavior, particularly examining reaction pathways, LBV, major species time profiles, and IDTs, to enhance kinetic models for engine applications.

Osswald et al. (2007) analyzed the combustion behavior of ethyl and methyl esters by utilizing molecular-beam mass spectrometry (MB-MS) for measuring the concentrations of key intermediate and major species in flat flames. The decomposition pathways of methyl acetate indicated the formation of formaldehyde (H_2CO) and emphasized the importance

of quantitatively assessing formaldehyde emissions in biodiesel formulations containing methyl esters. Westbrook et al. (2009) proposed a model for small alkyl esters by using the functional group similarities to constrain unimolecular decomposition and H-atom abstraction reactions. Dabbagh et al. (2013) examined the addition of methyl acetate to gasoline and observed an increase in the research octane number, with minimal impact on the Reid vapor pressure. Yang et al. (2015) analyzed the oxidation and pyrolysis of methyl acetate using the MB-MS and a low-pressure flat flame burner and developed a kinetic model for methyl acetate. Their experimental findings revealed that methyl acetate oxidation produces acids, ketones, and aldehydes. Ren et al. (2017) studied the pyrolysis and combustion behavior of methyl acetate in a shock tube (ST), employing laser absorption spectroscopy to analyze the time histories of H_2O, OH, CO_2, and CO, thereby gaining insights into its reaction pathways. The mechanism developed by Yang et al. (2015) successfully predicted the evolution of CO and CO_2 concentrations during the thermal decomposition of methyl acetate.

Wang et al. (2014) investigated the LBV of esters using counterflow (CF) flame experiments. The LBV values of methyl acetate/air mixtures were found to be lower than those of methyl formate, primarily due to increased ketene formation during the decomposition of the $CH_2C(O)OCH_3$ radical. Ahmed et al. (2019) conducted a comprehensive study on small alkyl esters by evaluating IDTs in a ST, analyzing oxidation behavior in a jet-stirred reactor, and measuring LBVs using the heat-flux (HF) technique. They developed a chemical kinetic mechanism for ethyl acetate and methyl acetate, with LBV predictions closely matching experimental results. Kim et al. (2019) carried out experiments to measure the LBV for 2-methylfuran, methyl acetate, and ethanol using the spherically expanding flame (SEF) method at 428 K under atmospheric pressure. The results showed that 2-methylfuran and ethanol exhibited similar LBV values, both higher than that of methyl acetate. Lubrano Lavadera et al. (2022) experimentally measured the LBV of methyl acetate over a mixture temperature range of 298 - 348 K and equivalence ratios from 0.7 to 1.5 using the HF method. They also developed a detailed chemical kinetic model that showed good agreement with experimental results for IDTs (Ahmed et al. 2019), LBVs (Wang et al. 2014; Lubrano Lavadera et al. 2022), and species profiles (Ahmed et al. 2019). Table 1 presents a summary of the reported LBVs of methyl acetate/air mixtures obtained using various experimental techniques across different mixture temperatures and equivalence ratios.

As shown in Table 1, the measurements of LBVs for methyl acetate/air mixtures were conducted at mixture temperatures varying from 298 to 428 K across different ɸ under atmospheric pressure conditions. However, typical mixture temperatures following the compression process in various engineering systems of practical relevance, including internal combustion engines, are significantly higher than 428 K. All previous chemical kinetic

Table 1. Summary of LBV reported by various researchers for methyl acetate/air mixtures.

Author	Method	ɸ	T_u (K)
Wang et al. (2014)	CF	0.7 - 1.5	333
Ahmed et al. (2019)	HF	0.7 - 1.4	298, 338
Kim et al. (2019)	SEF	0.8 - 1.5	428
Lubrano Lavadera et al. (2022)	HF	0.7 - 1.5	298 - 348

ɸ - Equivalence ratios, T_u - Mixture temperature.

models have been developed based on the available LBV measurements at these mixture temperatures, and their predictions generally align well with the reported experimental data. However, assessing the combustion performance of these models at elevated temperatures relevant to engine operating conditions is crucial for validating their accuracy and reliability in practical applications.

A detailed comparison of the existing experimental studies shows that the existing LBV data is limited to lower mixture temperatures ($T_u \leq 428$ K). The present work significantly extends the understanding of the LBV of methyl acetate/air mixtures and thereby improved understanding of the combustion behavior by reporting the experimental measurements over an elevated mixture temperature range of 367 - 714 K and equivalence ratios from 0.7 to 1.4 using the externally heated diverging channel method. The exploration of LBV behavior at such high mixture temperature conditions helps address a critical gap in the literature and provides accurate LBV data for the validation of chemical kinetic models under these mixture conditions, which are relevant to the practical combustion systems.

Methodology

Computational details

LBV predictions for methyl acetate/air mixtures were obtained using detailed chemical kinetic mechanisms developed by Diévart et al. (2013), Ahmed et al. (2019), and Lubrano Lavadera et al. (2022), using Cantera software (Goodwin et al. 2018). The species and reaction details for these models are summarized in Table 2. For premixed flame simulations, the "FreeFlame" object was utilized, with refinement criteria set as ratio = 3, curve = 0.075, and slope = 0.075, which control the grid point distribution across a flame domain width of 0.03 m. The mixture-averaged transport model was employed to evaluate gas-phase properties such as viscosity, diffusion coefficients, and thermal conductivity. Simulations were performed across a range of equivalence ratios and temperatures under atmospheric pressure conditions.

Experimental details

Figure 1 presents the detailed configuration of the diverging channel and the schematic of the experimental setup used in this study. The required airflow is monitored and controlled using a command module and an air mass flow controller (flow rate range: 0 - 5 LPM, accuracy: ±1.5%). Liquid fuel is supplied via a high-precision syringe pump. The incoming air is preheated by an air preheater and directed through a heated tube. Methyl acetate (supplied by CHEMICAL CENTER, purity: 99.34% based on gas chromatography analysis) is injected into the preheated air using the syringe pump. As the liquid fuel enters the "J" junction of the heated air line, it vaporizes due to the elevated

Table 2. Details of chemical kinetic models.

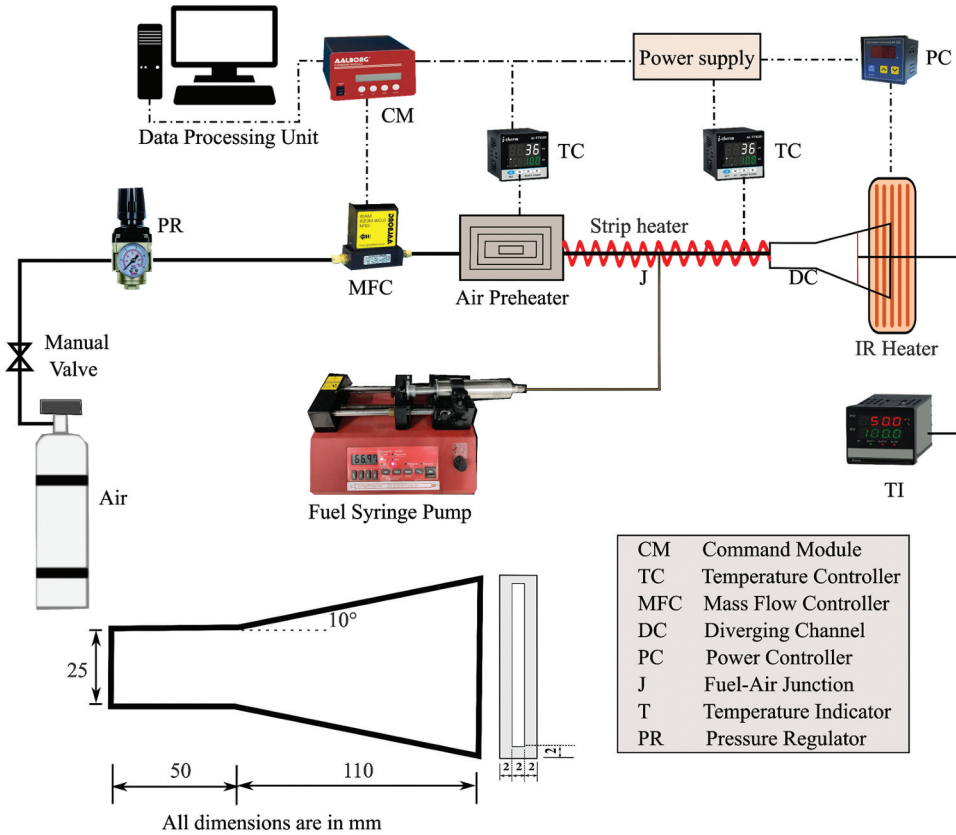| Model	# Species	# Reactions
Diévart (2013)	256	1925
Ahmed (2019)	506	2809
Lubrano Lavadera (2022)	284	3443

Figure 1. Details of the diverging channel and layout of the experimental setup.

air temperature, forming a uniform fuel-air vapor mixture. To avoid fuel condensation, the temperature of the fuel-air mixture line is maintained approximately 10 K above the boiling point of the liquid fuel. This is achieved using strip heaters, temperature controllers, solid-state relays, and thermocouples. The homogeneous vapor mixture is introduced into the diverging channel and ignited at the open end. Upon ignition, the flame propagates through the diverging channel, consuming the reactants until it stabilizes at a location where the incoming mixture flow velocity balances the flame burning velocity. The stabilized planar flame forms at this equilibrium point, governed by the balance among mixture flow velocity, burning velocity, and mixture temperature (Akram and Kumar 2011). An external infrared ceramic heater is positioned below the channel at the open end, overlapping by approximately 20 mm (as shown in Figure 1), to establish a positive temperature gradient along the flow direction. This also helps compensate for heat losses to the channel walls and supports near-adiabatic flame conditions (Berwal, Kumar, and Kumar 2023; Kumar, Singhal, and Kumar 2021).

Figure 2 displays a photograph of a stabilized planar flame formed at an inlet mixture velocity of 1.4 m/s and equivalence ratio, $\phi = 1.0$. The LBV (S_u) of the methyl acetate/air mixture is determined from the stabilized planar flame using the modified mass conservation equation (Equation (1)).
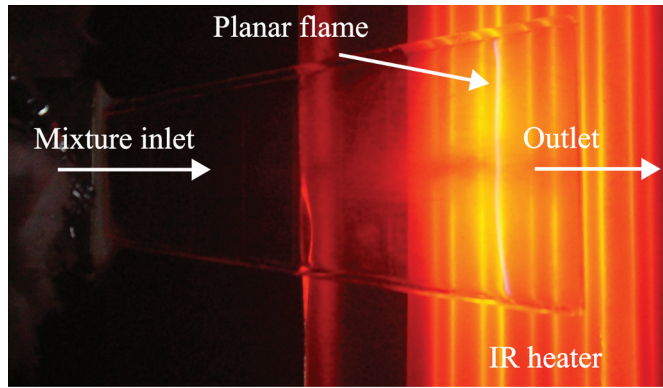
Figure 2. Stabilized planar flame for U_{in} of 1.4 m/s at stoichiometric mixture conditions.

$$S_u = U_{in} \times \frac{T_u}{T_{in}} \times \frac{A_{in}}{A_f} \tag{1}$$

Here, U_{in}, T_{in}, and A_{in} represent the mixture velocity, unburned mixture temperature, and cross-sectional area at the inlet section, respectively, while T_u and A_f correspond to unburned gas temperature at the flame location and flame cross-sectional area.

Uncertainty analysis

The uncertainty in LBV measurements depends on the accuracy of flame area, unburned mixture temperature, and inlet mixture velocity measurements, as shown in Eqn. 1. The total uncertainty for methyl acetate/air LBV measurements is estimated using the error propagation method (Varghese et al. 2018; Varghese, Kolekar, and Kumar 2019). The uncertainty in unburned mixture temperature arises from the K-type thermocouple, which offers an accuracy of 0.75% of the measured value or ±2.2 K. The flame area measurement uncertainty is ±0.71 mm². The inlet mixture velocity uncertainty is determined by the precision of the air mass flow controller (Aalborg, GFC 17) and the accuracy of the infusion syringe pump used to control fuel flow. The air mass flow controller has a precision of ±1.5% of its maximum range, while the syringe pump has an accuracy of ±1%. Considering all contributing factors, the overall uncertainty in LBV measurement for methyl acetate/air mixtures is estimated to be less than ±5%.

Results and discussions

Effect of temperature ratio on LBV

Figure 3 shows the effect of mixture temperature on the LBV of methyl acetate/air mixtures, comparing the present experimental results with existing data across a range of equivalence ratios and evaluating model predictions against measured values. The x-axis represents the nondimensional temperature ratio, $T_u/T_{u,0}$, where $T_{u,0}$ is the reference temperature taken as 300 K. The relationship between mixture temperature (T_u) and LBV (S_u) follows the power-law correlation: $S_u = S_{u,0} \times (T_u/T_{u,0})^\alpha$, where α is the temperature exponent and $S_{u,0}$ is the LBV at the reference temperature.
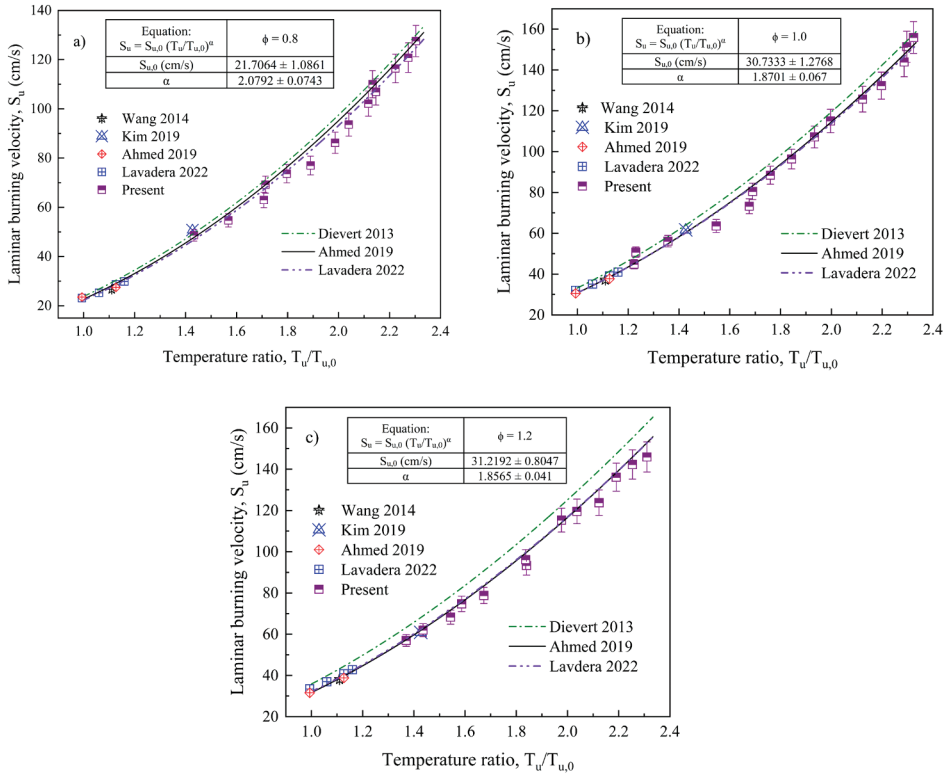
Figure 3. Variation of LBV with mixture temperature for the mixture equivalence ratios of a) φ = 0.8, b) φ = 1.0, and c) φ = 1.2.

The present measurements are fitted using this power-law correlation, and the resulting coefficients (α and $S_{u,0}$) for various equivalence ratios are summarized in the inset table within Figure 3. An increase in $T_u/T_{u,0}$ leads to higher LBV values, attributed to enhanced mixture diffusivity, reactivity, and reaction rates. As shown in the figure, the kinetic models proposed by Ahmed (2019) and Lubrano Lavadera (2022) show good agreement with both the current and previously reported measurements across a range of temperature and φ. In contrast, the Diévart (2013) model overpredicts the LBV under varying temperature at rich mixture equivalence ratios (φ = 1.2).

Effect of equivalence ratios on LBV at various mixture temperatures

Figure 4(a) presents a comparison of the existing experimental data with present LBV measurements and predictions from various chemical kinetic models at mixture temperatures of 298 and 348 K. At 348 K, the present results show good agreement with the LBV data reported by Lubrano Lavadera et al. (2022) across all φ. Conversely, at 298 K, the current measurements align closely with the data reported by Ahmed et al. (2019). Under stoichiometric conditions, the LBV measured in this study increases from 30.35 cm/s at 298 K to 40.57 cm/s at 348 K, demonstrating a clear temperature dependence. The kinetic models by Ahmed (2019) and Lubrano Lavadera (2022) accurately capture this trend,
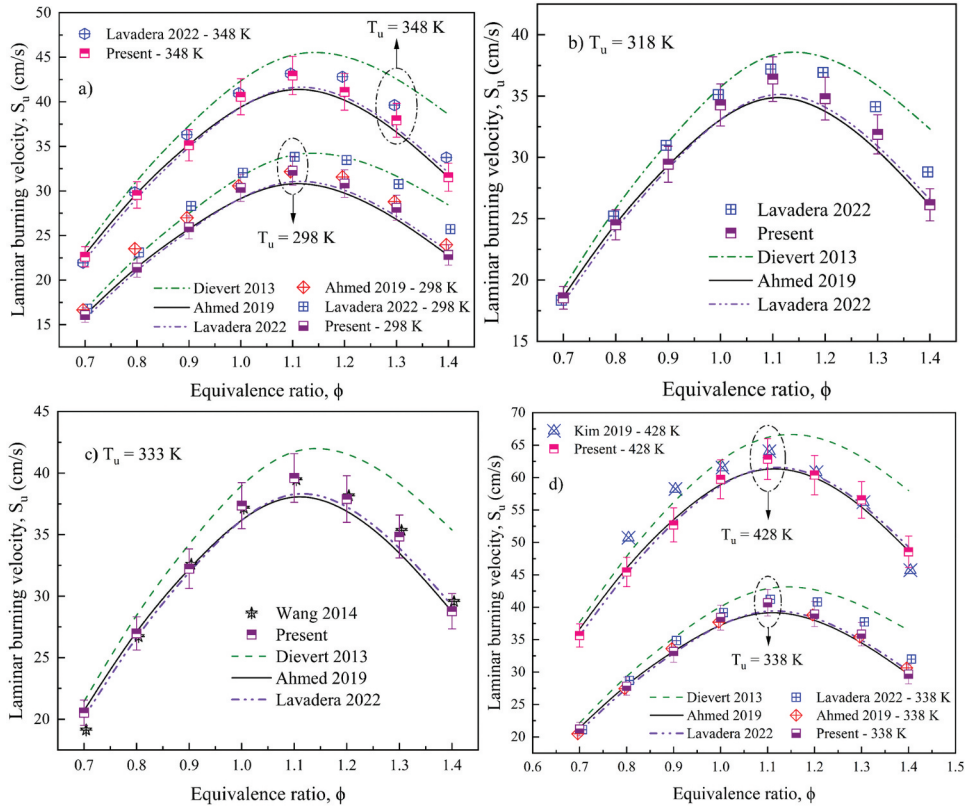
Figure 4. Variation of LBV with ɸ at: a) 298 and 348 K, b) 318 K, c) 333 K, and d) 338 and 428 K.

showing good agreement with the experimental results at both temperatures. In contrast, the Diévart et al. (2013) model shows overpredictions in the fuel-rich mixture conditions.

Figure 4(b,c) present a comparison between the present experimental measurements and those reported by Lubrano Lavadera et al. (2022) and Wang et al. (2014) at mixture temperatures of 318 K and 333 K, respectively. Across the range of ɸ, the current results show good agreement with both datasets.

Figure 4d compares LBV predictions from models with experimental data at 338 K and 428 K. At 338 K, the LBV values predicted by the Ahmed (2019) and Lubrano Lavadera (2022) models closely match the present measurements over various ɸ. At 428 K, Kim et al. (2019), using the SEF method, reported slightly higher LBV values in fuel-lean mixtures, while their data show close alignment with the present results under fuel-rich conditions. At mixture temperatures of 338 K and 428 K, the LBV predictions from Lubrano Lavadera (2022) and Ahmed (2019) show good agreement with the experimental results. In contrast, the Diévart et al. (2013) model overpredicts the LBV under fuel-rich conditions when compared to both the present study and previously reported measurements.

Across all investigated mixture temperatures (298 - 428 K), the LBV displays a parabolic dependence on the equivalence ratio, with a peak occurring at ɸ = 1.1. Increasing the mixture temperature from 338 K to 428 K leads to a rise in the peak LBV from 40.70 cm/s to 62.83 cm/s.
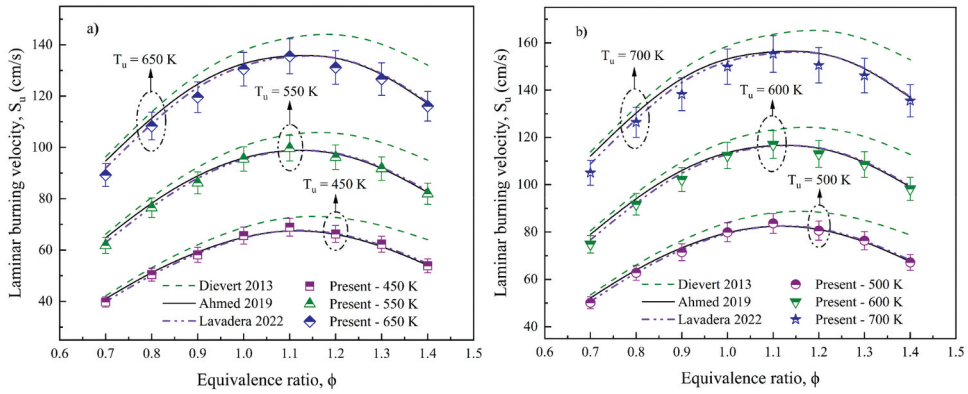
Figure 5. Variation of LBV with φ at elevated mixture temperatures: a) 450, 550, and 650 K; b) 500, 600, and 700 K.

Effect of elevated mixture temperatures on LBV

Figures 5(a,b) show the effect of elevated mixture temperature on the LBV of methyl acetate/air mixtures, along with a comparison to predictions from kinetic models. At stoichiometric equivalence ratios, the LBV increased by approximately 97% as the temperature increased from 450 K to 650 K. Similarly, the peak LBV exhibited an increase of about 86% with a temperature rise from 500 K to 700 K. The LBV predictions from the kinetic models developed by Ahmed (2019) and Lubrano Lavadera (2022) show close agreement with the present experimental data.

LBV comparison of acetates

Figure 6(a) presents a comparison of the experimentally measured LBV data reported by Konnov, Chen, and Lubrano Lavadera (2023) for various acetates at a mixture temperature of 338 K. Under fuel-lean conditions, the LBV follows the trend: methyl acetate < propyl
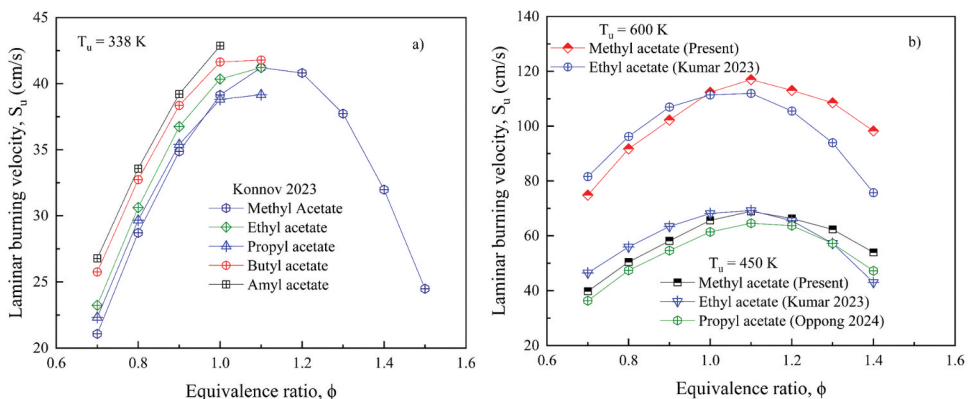

Figure 6. Experimental comparison of LBV of acetate at different mixture temperatures at a) 338 K and b) 450 K and 600 K.

acetate < ethyl acetate < butyl acetate < amyl acetate. Interestingly, at specific equivalence ratios, LBV generally increases with carbon chain length, with the exception of propyl acetate. Across all equivalence ratios, propyl acetate exhibits lower LBV values than ethyl acetate, and at $\phi = 1.1$, its LBV is even lower than that of methyl acetate. At $\phi = 1.0$, the LBV of amyl acetate is higher than methyl acetate by ~3.7 cm/s.

Figure 6(b) presents the variation of LBV with ϕ for methyl acetate, compared with existing experimental results for ethyl acetate (Kumar, Padhi, and Kumar 2023) and propyl acetate (Oppong et al. 2024) at mixture temperatures of 450 K and 600 K. At 450 K, under fuel-lean to stoichiometric conditions, ethyl acetate exhibits higher LBV values than methyl and propyl acetate. However, at $\phi = 1.4$, the trend reverses, with LBV values following the order: methyl acetate > propyl acetate > ethyl acetate. A similar trend is observed for methyl and ethyl acetate at the elevated mixture temperature of 600 K. Ethyl acetate exhibits higher LBV values in fuel-lean mixtures; however, methyl acetate shows higher LBV values for stoichiometric to fuel-rich conditions.

Variation of temperature exponent with equivalence ratios

The temperature exponent (α) in the power-law correlation (Equation (2)) quantifies the sensitivity of the LBV (S_u) to changes in the unburned mixture temperature (T_u).

$$S_u = S_{u,0} \left(\frac{T_u}{T_{u,0}} \right)^\alpha \tag{2}$$

Where, $S_{u,0}$ and S_u represent the LBV at the unburned mixture temperatures, $T_{u,0}$ and T_u, respectively.

Figure 7 compares the temperature exponents (α) obtained from the present measurements and the predictions of chemical kinetic models. The temperature exponent
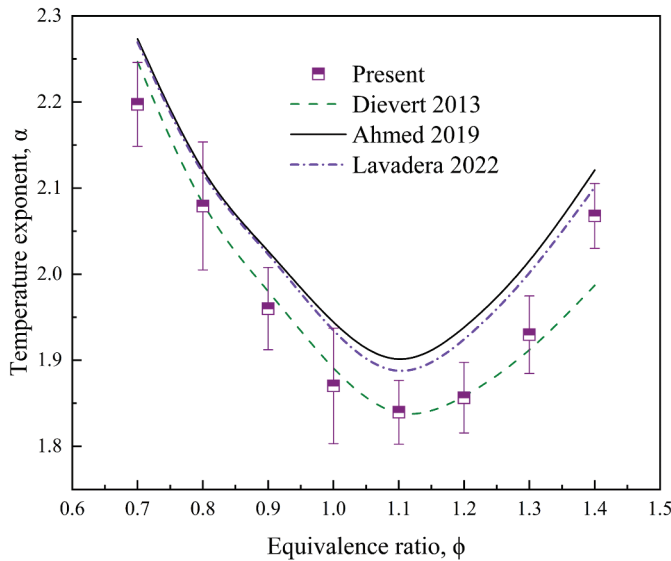

Figure 7. Variation of temperature exponent (α) with ϕ for methyl acetate/air mixtures.

reaches its lowest value at slightly rich (ϕ = 1.1) mixtures and increases for both fuel-lean and fuel-rich conditions. The maximum LBV occurs under slightly rich mixture conditions (ϕ = 1.1), where the adiabatic flame temperature also reaches its peak. Under these conditions, dissociation reactions become more significant, moderating the rate of LBV change with temperature and resulting in lower α values. In contrast, lean and rich mixtures exhibit lower adiabatic flame temperatures, reducing the influence of dissociation reactions. As a result, α values are relatively higher in these conditions, indicating greater LBV sensitivity to changes in unburned gas temperature. This behavior is consistent with the more pronounced variation in adiabatic flame temperature for lean and rich mixtures compared to near stoichiometric for a given increase in mixture temperature (Akram, Kumar, and Saxena 2013; Mohammad and Juhany 2019; Shinde, Fulzele, and Kumar 2024).

Additionally, at a slightly rich equivalence ratio (ϕ = 1.1), radical production is optimized due to a balanced proportion of fuel and oxidizer, resulting in reduced sensitivity of LBV to temperature changes. In contrast, under very lean (ϕ = 0.7) or very rich (ϕ = 1.4) conditions, limited radical formation makes the combustion process more temperature sensitive, leading to higher α values. This trend has also been reported in earlier studies for various fuel-air mixtures (Fulzele, Shinde, and Kumar 2025; Konnov et al. 2018; Rajesh and Prathap 2022). A higher temperature exponent reflects a stronger dependence of LBV on temperature, which is particularly important for high-temperature combustion systems where flame propagation and heat release characteristics are critically affected.

Sensitivity analysis

To understand the role of key elementary reactions influencing the LBV of methyl acetate/air mixtures at different mixture and temperature conditions, the normalized sensitivity coefficients are analyzed. The sensitivity analysis is performed using the Lubrano Lavadera (2022) kinetic model, considering accurate predictions obtained from this model, with respect to the present measurements.

Figure 8a compares the sensitivity of various reactions at 428 K and 700 K temperatures and stoichiometric mixture conditions (ϕ = 1.0). Both R12 (H + O_2 ⇌ O + OH) and R187 (CO + OH ⇌ CO_2 + H) reactions promote LBV by enhancing the radical pool. R12 contributes through chain branching, while R187 supports radical regeneration and heat release. Their sensitivities are higher at 428 K mixture temperature, where radical generation is limited and chain branching reactions are critical for sustaining combustion. At 700 K, their influence slightly decreases as other radical-producing reactions, such as, HCO or CH_3 decomposition become more dominant, shifting the combustion dynamics toward high-temperature-driven pathways. R192 (HCO + M ⇌ CO + H + M) is a radical-generating and chain-propagating reaction that decomposes HCO into CO and H, enhancing the mixture LBV. Its influence increases at higher temperatures due to enhanced thermal decomposition, while at 428 K, this reaction shows relatively weaker effect due to slower kinetics. Reactions R11 (H_2 + O ⇌ H + OH), R160 (CH_3 + HO_2 ⇌ CH_3O + OH), and R144 (CH_3 + O ⇌ CO + H + H_2) exhibit positive sensitivity coefficients, highlighting their supportive role in promoting LBV. Although their impact is relatively lower, when compared to key reactions like R12 and R187, they contribute through secondary radical-generation pathways. R11 and R160 show minimal change in sensitivity with increase in temperature.
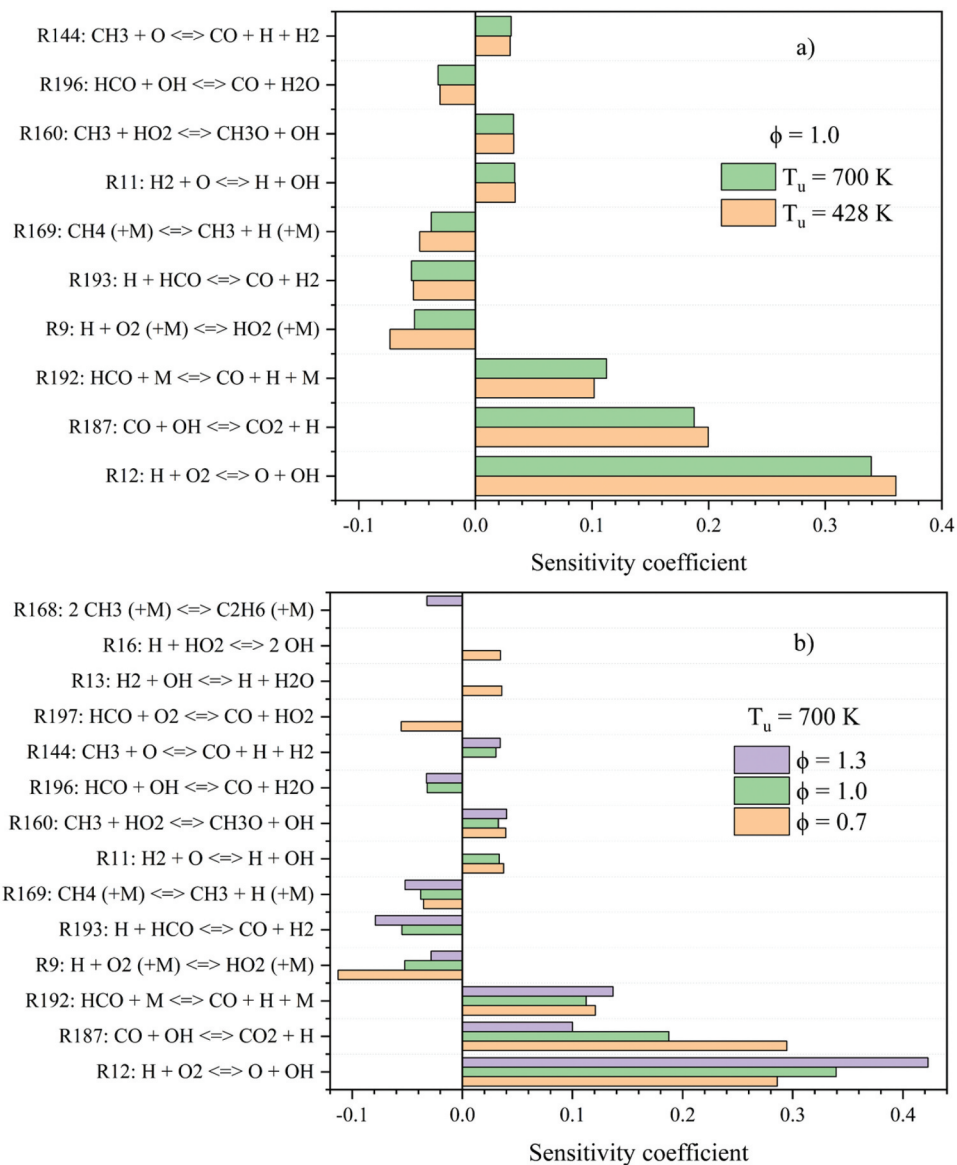
Figure 8. Normalized sensitivity coefficients for methyl acetate/air mixtures at a) 428 K and 700 K under stoichiometric conditions, and b) 700 K for different mixture equivalence ratios.

Reactions R9 ($H + O_2 + M \rightleftharpoons HO_2 + M$) and R169 ($CH_4 + M \rightleftharpoons CH_3 + H + M$) exhibit negative sensitivity coefficients. R9 acts as a chain-terminating reaction by consuming the reactive H atoms and forming less reactive HO_2 radicals. Its negative effect is more pronounced at 428 K, where radical availability is limited, and becomes slightly less significant at 700 K due to enhanced radical generation from other reactions. R169 further depletes the radicals by combining CH_3 and H to form stable CH_4, reducing overall flame reactivity. Reactions R193 ($H + HCO \rightleftharpoons CO + H_2$) and R196 ($HCO + OH \rightleftharpoons CO + H_2O$) show negative sensitivity coefficients, indicating their suppressive influence

on LBV by consuming the reactive radicals. R193 consumes H and HCO radicals to form CO and H_2 and exhibits a stronger negative sensitivity than R196, with minimal variation between 428 K and 700 K conditions. In contrast, R196 consumes HCO and OH radicals, shows a less negative sensitivity that becomes pronounced at 700 K. This implies it is the suppressive role of R196 with higher radical concentrations at elevated temperatures.

Figure 8b shows the sensitivity of key reactions to LBV at a mixture temperature of 700 K for different equivalence ratios (φ = 0.7, 1.0, and 1.3), highlighting significant variations with φ. R12 shows a clear and strong increase in sensitivity as φ increases from lean (φ = 0.7) to rich (φ = 1.3). This indicates that radical branching via O and OH production becomes increasingly important in richer mixtures, where sustaining chain reactions relies more on effective radical generation due to reduced oxygen availability. In contrast, R187 displays a decreasing trend in sensitivity with increasing equivalence ratio. Its role in regenerating H radicals through CO oxidation is more pronounced under lean to stoichiometric conditions, where OH is more available. Under rich conditions, diminished OH concentrations reduce the effectiveness of this pathway, leading to a weaker contribution to LBV. R192 exhibits a non-monotonic sensitivity trend, with its coefficient being higher at φ = 0.7 and φ = 1.3, but lower at φ = 1.0. This suggests that HCO decomposition into CO and H plays a greater role at extreme mixture conditions, where either high oxygen availability (lean) or high intermediate accumulation (rich) enhances its pathway. Similarly, R160 shows a similar non-monotonic pattern, with a lower sensitivity at φ = 1.0 and higher values at φ = 0.7 and 1.3. This behavior indicates that the formation of OH radicals from CH_3 and HO_2 is more impactful under lean and rich conditions, likely due to increased concentrations of CH_3 in rich conditions and HO_2 in lean conditions.

Reactions R9, R169, R193, and R196, all show negative sensitivity coefficients, indicating their roles in suppressing LBV by consuming the pool of reactive radicals. R9 has the strongest negative effect at φ = 0.7, where it converts H radicals into HO_2, significantly reducing the chain propagation. Its impact decreases with increasing φ as the availability of oxygen scarce in rich mixtures, making this O_2-dependent termination path less dominant. R169 exhibits an increasingly negative sensitivity with rising φ. Its suppressive effect is most notable at φ = 1.3, where high CH_3 and H concentrations promote recombination into stable CH_4, depleting the radical pool essential for LBV enhancement. R193 is absent at φ = 0.7, indicating that it plays a negligible role under lean conditions. However, it shows strong negative sensitivity at φ = 1.0 and 1.3, with greater suppression in rich mixtures due to increased HCO and H radical concentrations, which intensify the radical-consuming effect. R196 displays a moderate negative sensitivity. As radical concentrations grow in rich mixtures, this reaction more effectively consumes HCO and OH, further reducing the mixture LBV at these conditions.

Sensitivity analysis shows that none of the top 10 reactions across different mixture equivalence ratios (φ = 0.7, 1.0, and 1.3) and mixture temperatures (428 K and 700 K) involve methyl acetate or its primary radicals. This suggests that the combustion behavior of methyl acetate is largely governed by small (C_0 - C_4) species chemistry rather than fuel-specific decomposition reactions. A similar observation was reported by Lubrano Lavadera et al. (2022), based on sensitivity analysis at 298 K for φ = 0.8, 1.0, and 1.3. The study concluded that models focusing on C_0 - C_4 reaction pathways adequately describe the consumption of methyl acetate derived intermediates such as CH_3OCO, CH_3CO_2, and CH_2

CO (ketene). The effect of elevated mixture temperatures on the reaction pathway is discussed in the supplementary material.

Conclusions

This study investigates the laminar burning velocity (LBV) of methyl acetate/air mixtures over an elevated temperature range of 367 - 714 K and equivalence ratios (φ) from 0.7 to 1.4, using the externally heated diverging channel method. The experimental results are compared with existing measurements and with predictions from chemical kinetic models developed by Ahmed (2019), Lubrano Lavadera (2022), and Diévart (2013), across various temperatures and equivalence ratios. The present measurements show good agreement with previously reported data over a broad range of conditions. The kinetic models by Ahmed (2019) and Lubrano Lavadera (2022) demonstrate strong predictive performance, aligning well with both the existing and current measurements at elevated mixture temperatures. In contrast, the model by Diévart et al. (2013) tends to overpredict LBV values, under fuel-rich conditions. Across all tested temperatures, the LBV exhibits a parabolic trend with a maximum at a slightly rich equivalence ratio (φ = 1.1), a behavior also captured by the models. At φ = 1.0, the LBV increases by around 97% as the mixture temperature rises from 450 K to 650 K. Additionally, the peak LBV increases by about 86% when the temperature is raised from 500 K to 700 K, emphasizing the strong temperature dependence of flame speed. Sensitivity analysis indicates that the combustion chemistry of methyl acetate/air mixtures is primarily governed by reactions involving C_0 - C_4 species.

Disclosure statement

No potential conflict of interest was reported by the author(s).

Funding

References

Ahmed, A., W. J. Pitz, C. Cavallotti, M. Mehl, N. Lokachari, E. J. Nilsson, J. Y. Wang, A. A. Konnov, S. W. Wagnon, B. Chen, et al. 2019. Small ester combustion chemistry: Computational kinetics and experimental study of methyl acetate and ethyl acetate. *Proc. Combust. Inst.* 37 (1):419–28. doi: 10. 1016/j.proci.2018.06.178.

Akram, M., and S. Kumar. 2011. Experimental studies on dynamics of methane–air premixed flame in meso-scale diverging channels. *Combust Flame* 158 (5):915–24. doi:10.1016/j.combustflame. 2011.02.011.

Akram, M., S. Kumar, and P. Saxena. 2013. Experimental and computational determination of laminar burning velocity of liquefied petroleum gas-air mixtures at elevated temperatures. *J. Eng. Gas Turbines Power* 135 (9):091501. doi: 10.1115/1.4024798.

Berwal, P., S. Kumar, and S. Kumar. 2023. Laminar burning velocity measurement of CH4/H2/ NH3-air premixed flames at high mixture temperatures. *Fuel* 331:125809. doi:10.1016/j.fuel.2022. 125809.

Coniglio, L., H. Bennadji, P. A. Glaude, O. Herbinet, and F. Billaud. 2013. Combustion chemical kinetics of biodiesel and related compounds (methyl and ethyl esters): Experiments and modeling–advances and future refinements. *Prog. Energy Combust. Sci.* 39 (4):340–82. doi:10.1016/j.pecs.2013.03.002.

Culaba, A. B., A. P. Mayol, J. L. G. San Juan, A. T. Ubando, A. A. Bandala, R. S. Concepcion II, M. Alipio, W. H. Chen, P. L. Show, and J. S. Chang. 2023. Design of biorefineries towards carbon neutrality: A critical review. *Bioresource. Technol.* 369:128256. doi: 10.1016/j.biortech.2022.128256.

Curran, H. J. 2019. Developing detailed chemical kinetic mechanisms for fuel combustion. *Proc. Combust. Inst.* 37 (1):57–81. doi: 10.1016/j.proci.2018.06.054.

Dabbagh, H. A., F. Ghobadi, M. R. Ehsani, and M. Moradmand. 2013. The influence of ester additives on the properties of gasoline. *Fuel* 104:216–23. doi:10.1016/j.fuel.2012.09.056.

Diévart, P., S. H. Won, J. Gong, S. Dooley, and Y. Ju. 2013. A comparative study of the chemical kinetic characteristics of small methyl esters in diffusion flame extinction. *Proc. Combust. Inst.* 34 (1):821–29. doi:10.1016/j.proci.2012.06.180.

Fulzele, A., V. Shinde, and S. Kumar. 2025. Experimental investigation on laminar burning velocity of iso-Octane/Air mixtures at elevated pressures and temperature conditions. *Fuel* 401:135940. doi: 10.1016/j.fuel.2025.135940.

Goodwin, D. G., R. L. Speth, H. K. Moffat, and B. W. Weber. 2018. Cantera: An object-oriented software toolkit for chemical kinetics, thermodynamics, and transport processes. *Zenodo*. doi: 10.5281/zenodo.4527812.

IEA. 2024. World Energy Outlook 2024, IEA, Paris 2024. Licence: CC BY 4.0 (report); CC BY NC SA 4.0 (Annex A). https://www.iea.org/reports/world-energy-outlook-2024.

Kim, G., B. Almansour, S. Park, A. Terracciano, S. Vasu, K. Zhang, S. Wagnon, and W. Pitz. 2019. Laminar burning velocities of high-performance fuels relevant to the Co-optima initiative. *SAE. Int. J. Adv. Curr. Pract. Mobil.* 1 (2019–01–0571):1139–47. doi: 10.4271/2019-01-0571.

Konnov, A. A., J. Chen, and M. L. Lavadera. 2023. Measurements of the laminar burning velocities of small alkyl esters using the heat flux method: A comparative study. *Combust Flame* 255:112922. doi: 10.1016/j.combustflame.2023.112922.

Konnov, A. A., A. Mohammad, V. R. Kishore, N. I. Kim, C. Prathap, and S. Kumar. 2018. A comprehensive review of measurements and data analysis of laminar burning velocities for various fuel+ air mixtures. *Prog. Energy Combust. Sci.* 68:197–267. doi: 10.1016/j.pecs.2018.05.003.

Kumar, R., U. P. Padhi, and S. Kumar. 2023. Laminar burning velocity measurements of ethyl acetate at higher mixture temperatures. *Fuel* 338:127278. doi: 10.1016/j.fuel.2022.127278.

Kumar, R., A. Singhal, and S. Kumar. 2021. Laminar burning velocity measurements of iso-octane+ air mixtures at higher unburnt mixture temperatures. *Fuel* 288:119652. doi:10.1016/j.fuel.2020.119652.

Lai, J. Y., K. C. Lin, and A. Violi. 2011. Biodiesel combustion: Advances in chemical kinetic modeling. *Prog. Energy Combust. Sci.* 37 (1):1–14. doi: 10.1016/j.pecs.2010.03.001.

Lam, K. Y., D. F. Davidson, and R. K. Hanson. 2012. High-temperature measurements of the reactions of OH with small methyl esters: Methyl formate, methyl acetate, methyl propanoate, and methyl butanoate. *J. Phys. Chem. A* 116 (50):12229–41. doi:10.1021/jp310256j.

Lavadera, M. L., S. Li, C. Brackmann, and A. A. Konnov. 2022. Experimental and modeling study of NO formation in methyl acetate+ air flames. *Combust Flame* 242:112213. doi:10.1016/j.combustflame.2022.112213.

Mohammad, A., and K. A. Juhany. 2019. Laminar burning velocity and flame structure of DME/methane+ air mixtures at elevated temperatures. *Fuel* 245:105–14. doi: 10.1016/j.fuel.2019.02.085 .

Oppong, F., Y. Liu, X. Li, C. Xu, and Y. Li. 2024. The laminar burning velocity of propyl acetate at high pressures and temperatures. *Fuel* 375:132600. doi: 10.1016/j.fuel.2024.132600.

Oppong, F., C. Xu, X. Li, and Z. Luo. 2022. Esters as a potential renewable fuel: A review of the combustion characteristics. *Fuel Process Technol.* 229:107185. doi:10.1016/j.fuproc.2022.107185.

Osswald, P., U. Struckmeier, T. Kasper, K. Kohse-Höinghaus, J. Wang, T. A. Cool, N. Hansen, and P. R. Westmoreland. 2007. Isomer-specific fuel destruction pathways in rich flames of methyl acetate and ethyl formate and consequences for the combustion chemistry of esters. *J. Phys. Chem. A* 111 (19):4093–101. doi:10.1021/jp068337w.

Rajesh, N., and C. Prathap. 2022. Investigation on the laminar burning velocity and flame stability of premixed n-dodecane-air mixtures at elevated pressures and temperatures. *Fuel* 318:123347. doi: 10.1016/j.fuel.2022.123347.

Ren, W., K. Y. Lam, D. F. Davidson, R. K. Hanson, and X. Yang. 2017. Pyrolysis and oxidation of methyl acetate in a shock tube: A multi-species time-history study. *Proc. Combust. Inst.* 36 (1):255–64. doi:10.1016/j.proci.2016.05.002.

Rial, R. C. 2024. Biofuels versus climate change: Exploring potentials and challenges in the energy transition. *Renew. Sustain. Energy Rev.* 196:114369. doi: 10.1016/j.rser.2024.114369.

Shinde, V., A. Fulzele, and S. Kumar. 2024. Investigation on laminar burning velocity measurements of premixed ethane-air mixture at higher pressure and temperature conditions. *Fuel* 358:130175. doi: 10.1016/j.fuel.2023.130175.

Sikiru, S., K. J. Abioye, H. B. Adedayo, S. Y. Adebukola, H. Soleimani, and M. Anar. 2024. Technology projection in biofuel production using agricultural waste materials as a source of energy sustainability: A comprehensive review. *Renew. Sustain. Energy Rev.* 200:114535. doi:10.1016/j.rser.2024.114535.

Tan, T., X. Yang, C. M. Krauter, Y. Ju, and E. A. Carter. 2015. Ab initio kinetics of hydrogen abstraction from methyl acetate by hydrogen, methyl, oxygen, hydroxyl, and hydroperoxy radicals. *J. Phys. Chem. A* 119 (24):6377–90. doi:10.1021/acs.jpca.5b03506.

Varghese, R. J., H. Kolekar, V. Hariharan, and S. Kumar. 2018. Effect of CO content on laminar burning velocities of syngas-air premixed flames at elevated temperatures. *Fuel* 214:144–53. doi:10.1016/j.fuel.2017.10.131.

Varghese, R. J., H. Kolekar, and S. Kumar. 2019. Laminar burning velocities of H2/CO/CH4/CO2/N2-air mixtures at elevated temperatures. *Int. J. Hydrogen Energy* 44 (23):12188–99. doi:10.1016/j.ijhydene.2019.03.103.

Wang, Y. L., D. J. Lee, C. K. Westbrook, F. N. Egolfopoulos, and T. T. Tsotsis. 2014. Oxidation of small alkyl esters in flames. *Combust Flame* 161 (3):810–17. doi:10.1016/j.combustflame.2013.09.013.

Westbrook, C. K., W. J. Pitz, P. R. Westmoreland, F. L. Dryer, M. Chaos, P. Oßwald, K. Kohse-Höinghaus, T. A. Cool, J. Wang, B. Yang, et al. 2009. A detailed chemical kinetic reaction mechanism for oxidation of four small alkyl esters in laminar premixed flames. *Proc. Combust. Inst.* 32 (1):221–28. doi:10.1016/j.proci.2008.06.106.

Yang, X., D. Felsmann, N. Kurimoto, J. Krüger, T. Wada, T. Tan, E. A. Carter, K. Kohse-Höinghaus, and Y. Ju. 2015. Kinetic studies of methyl acetate pyrolysis and oxidation in a flow reactor and a low-pressure flat flame using molecular-beam mass spectrometry. *Proc. Combust. Inst.* 35 (1):491–98. doi:10.1016/j.proci.2014.05.058.